We are IntechOpen, the world's leading publisher of Open Access books

Built by scientists, for scientists

6,900
Open access books available

185,000
International authors and editors

200M
Downloads

154
Countries delivered to

Our authors are among the

TOP 1%
most cited scientists

12.2%
Contributors from top 500 universities

CLARIVATE ANALYTICS
BOOK CITATION INDEX
INDEXED

WEB OF SCIENCE™

Selection of our books indexed in the Book Citation Index
in Web of Science™ Core Collection (BKCI)

Interested in publishing with us?
Contact book.department@intechopen.com

Numbers displayed above are based on latest data collected.
For more information visit www.intechopen.com

Multimodal Medical Image Registration and Fusion in 3D Conformal Radiotherapy Treatment Planning

Bin Li
South China University of Technology
China

1. Introduction

Medical image is the technique and process used to create images of the human body for medical science or clinical purposes, including medical medical procedures seeking to reveal, diagnose or examine disease. In the last 100 years, medical imaging technology has grown rapidly and drastically changed the medical profession. Now, physicians can use the images obtained by different medical imaging technologies to both diagnose and track the progress of illnesses and injuries. When 3D conformal radiotherapy planning (3D CRTP) is employed for tumor treatment, the relative position between the tumor and its adjacent tissues, should be obtained accurately. Generally, there are two main kinds of medical images which provide different information for diagnosis in 3D conformal radiotherapy planning (3D CRTP). They are "the anatomical images" and "the functional mages". The anatomical images, such as Computerized Tomography(CT), depict clearly primarily morphology of human body through the abundant texture, yet it is not very sensitive to the cancer. The functional mages, such as Positron Emission Tomography (PET), depict primarily information on the metabolism of the underlying anatomy. Therefore, the relative position between the tumor and its adjacent tissues could be obtained easily through analyzing the medical data sets which are fused the information of functional mages and anatomical images.

Many methods exist to perform image fusion. The very basic one is the high pass filtering technique. Later techniques are based on DWT, uniform rational filter bank, and so on. In this chapter, multimodal medical images are fused by applying wavelet transform with fusion rule of combining the local standard deviation and energy, which will be describe in detail in this chapter. Many documents presented a fusion method based on wavelet transform(Park J H et al., 2001), which is useful for image fusion. But the activity measure of the coefficients reflecting the significant information of multimodal medical images had not been considered in them. In clinic application, physicians are interested in the position signs of the tumor. The anatomical images depict clearly primarily morphology of human body through the abundant texture. So the local standard deviation is regarded as the activity measure of coefficients. Furthermore, the local energy reflects the absolute intensity of the signal change, and the large absolute intensity of the signal change reflect the obvious feature of the image. So the image feature is described in uniform by the local standard,

which reflects the definition. Therefore, the local standard deviation and energy standard are selected as the activity measure of the coefficients here.

In computer vision, multi-sensor image fusion is the process of combining relevant information from two or more images into a single image. The resulting image will be more informative than any of the input images. For multimodal medical images, the important thing is the fusion of multimodal images, while the registration is the basis for image fusion. Given two image sets acquired from the same patient but at different times or with different devices, image registration is the process of finding a geometric transformation between the two respective image-based coordinate systems that maps a point in the first image set to the point in the second set that has the same patient-based coordinates, i.e. represents the same anatomic location(David M. et al., 2003). This notion presupposes that the anatomy is the same in the two image sets, an assumption that may not be precisely true if, for example, the patient has had a surgical resection between the two acquisitions. The situation becomes more complicated if two image sets that reflect different tissue characteristics [e.g. computed tomography (CT) and positron emission tomography (PET)] are to be registered. The idea can still be used that, if a candidate registration matches a set of similar features in the first image to a set of features in the second image that are also mutually similar, it is probably correct. For example, according to the principle of mutual information, homogeneous regions of the first image set should generally map into homogeneous regions in the second set(David M. et al., 2003). Usually there are several registration methods for different organs or tissues, such as rigid registration, affine registration and elastic registration(M.Betke et al., 2003) (Maintz J.B.A. et al., 1998) (T. Blaffert et al., 2004). In clinical diagnosis, the application of registration methods are just a compromise among the calculation time, accuracy and robustness. Up to now, it is still a major challenge to develop a rapid and automatic registration method whose accuracy can reach to that of manual guided registration(David M. et al., 2003) (Stefan Klein et al., 2007). For the moving organs, non-rigid registration methods are needed because the position, size and shape of internal organs and tissues are affected by the involuntary and other physiological movements of patient. Among the non-rigid registration methods, the Free-Form Deformation(FFD) method(Bardinet E et al., 1996) based on B-splines can control local deformation and change of the control points. For hierarchical B-splines is more smooth and accurate than the common B-splines, so good performance can be achieved if it is applied for floating image deformation(Lee Seungyong et al., 1997) (Ruechert D. et al., 1999) (Ino Fumihiko et al., 2005) (Zhiyong Xie et al., 2004). Thus, the presented automatic fine registration method is designed based on the hierarchical B-splines in this chapter. In 3D CRTP, the key problem for the non-rigid registration method of medical image is that it is a task of very time-consuming calculation process, which is unable to meet the clinical requirement to real-time process. In the mean time, the image data sets in 3D CRTP are so mass that it is very difficult to fuse the information of multimodal sequence images in real time. Thus some optimization measures should be taken. In this chapter, the FFD and maximum mutual information algorithm used in the presented registration method are both non-linear algorithms, so it can be taken as a multi-objective nonlinear problem. Here, the gradient descent algorithm and maximum mutual information entropy criterion are used to accelerate the searching speed for FFD coefficients. Moreover, parallel computing(Yasuhiro K. et al., 2004) (S.K.Warfield et al., 1998) can potentially further increase matching and fusion efficiency, so the parallel matching and fusion technique based on high performance computation is used in this chapter.

From the aforementioned, in order to realize effectively and efficiently the automatic registration and fusion of multimodal medical images data, an image registration and fusion method in 3D CRTP is presented in detail in this chapter. This presented automatic registration method is based on hierarchical adaptive free-form deformation(FFD) algorithm and parallel computing, and the presented parallel multimodal medical image fusion method is based on wavelet transform with fusion rule of combining the local standard deviation and energy. This study demonstrates the superiority of the presented method.

2. Algorithm description of multimodal medical image registration and fusion

The steps of the presented algorithm are illustrated in Fig. 1, which can be described as follows: First given two image sets acquired from the same patient but at different times or with different devices, e.g. CT and PET. Then the ROI is extracted by using the C-V level sets algorithm, and feature points are matched automatically which is based on parallel computing method. Then, the global rough registration and automatic fine registration of the multimodal medical images is carried out by employing principal axes algorithm and a free-form deformation(FFD) method based on hierarchical B-splines. After the registration of multimodal images, their sequence images are fused by applying an image fusion method based on parallel computing and wavelet transform with the fusion rule of combining the local standard deviation and energy.
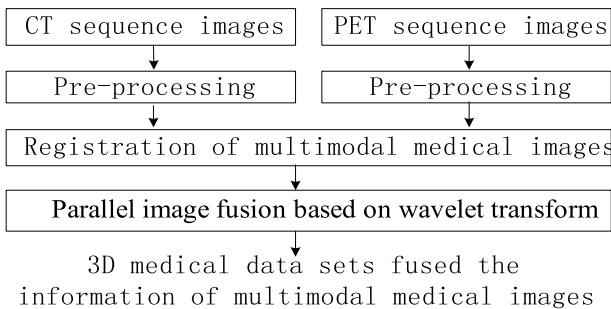
```
┌──────────────────────┐   ┌──────────────────────┐
│ CT sequence images   │   │ PET sequence images  │
└──────────┬───────────┘   └──────────┬───────────┘
           ▼                          ▼
┌──────────────────────┐   ┌──────────────────────┐
│   Pre-processing     │   │   Pre-processing     │
└──────────┬───────────┘   └──────────┬───────────┘
           ▼                          ▼
┌───────────────────────────────────────────────────┐
│     Registration of multimodal medical images     │
└───────────────────────┬───────────────────────────┘
                        ▼
┌───────────────────────────────────────────────────┐
│  Parallel image fusion based on wavelet transform  │
└───────────────────────┬───────────────────────────┘
                        ▼
        3D medical data sets fused the
    information of multimodal medical images
```

Fig. 1. Flow chart of the presented rapid registration and fusion method of multimodal medical image

3. Data preprocessing of medical images

In 3D CRTP, before the step of registration and fusion, scan data from PET and CT should be normalized or pre-processed according to the requirements of the next fusion step.

For the calculation of the fusion of PET and CT images, the standard uptake value(SUV) is frequently used for fluorodeoxyglucose(FDG) PET image to evaluate its uptake value quantitatively(S-C. Huang, 2000) (Aparna Kanakatte et al., 2007). In general, if there exists a tumor it will appear brighter than healthy cells in a PET image. This character is commonly used to identify healthy tissue from a tumor. Thus, the SUV is also named as the differential uptake ratio, or the differential absorption ratio, or the dose uptake ratio or the dose absorption ratio.

In order to obtain the tissue activity in each point, Bq/cc, units as measured by the PET/CT scanner, the pixel data is rescaled by tags "Rescale Slope" and "Rescale Intercept" available from the dicom header. The SUV is a useful quantitative way comparing tumors across different patients. For the calculation of SUV, the body weight of a patient is

commonly used, sometimes, physicians prefer to use body surface or lean body mass instead. The SUV for each voxel is calculated assuming $1cc = 1g$ and applying Eq.(1).

$$SUV = \frac{YW}{D} \qquad (1)$$

where W is the patient weight in kg; D is the injected dose at scan start (Bq); Y is the activity whose concentration in Bq / cc is calculated from Eq.(2).

$$Y = ax + b \qquad (2)$$

where x is the original pixel intensity value, a is the rescale slope and b is the rescale intercept for each image slice of the PET scan.

According to Aparna(Aparna Kanakatte et al., 2007), the higher the SUV is, the more aggressive the tumor is. The SUV is also used to distinguish the malignant tumor and benign tumor. An SUV of 2.5 is often considered as the threshold to distinguish benign and malignancy, however, the threshold value varies for different body organs, and if taking the breathing movement in account, the SUV will increase.

4. Registration of multimodal medical images

4.1 Flow chart for image registration

The presented image registration method applying adaptive FFD which is based on hierarchical B-splines algorithm is shown as Fig.2.
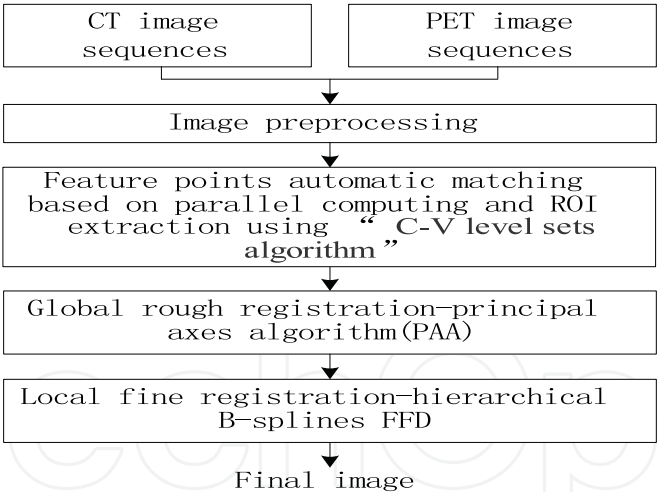

Fig. 2. Flow chart for image registration method applying adaptive FFD

The registration for medical images is a big challenge, this is because the position, size and shape of internal organs and tissues are affected by involuntary physiological movements and patient' motion when scanning, where various deformations are existent in the mean time, for example, the rigid motion of human body, the local elastic deformations of organs in motion. This will require the registration method be done about the global deformation at first, and then fine adjusting is conducted about local elastic deformation. Thus, registration process can be divided into two sub-process: one is the global rigid deformation by adopting principal axes algorithm, the other is the local elastic deformation by adopting adaptive FFD based on B-splines.

4.2 Measure of similarity for multimodal medical images

The mutual information[17,18] of multimodal medical images is taken as similarity index for registration, which is essentially the expression about the statistical characteristic of gray information between two images. An objective function can be used to define the similarity measure between the reference image and floating image.

Suppose the gray intensity of reference image is I_R, while that of the floating image is I_F, the information entropy for I_R is $H(I_R)$, it is $H(I_F)$ for I_F. Let $H(I_R,I_F)$ denote the combined information entropy of I_R and I_F, then the mutual information of two images is defined as follows:

$$MI(I_R,I_F) = H(I_R) + H(I_F) - H(I_R,I_F) \qquad (3)$$

When two images are strictly matched, $MI(I_R,I_F)$ will be the maximum. For the registration of the multimodal medical images although the two images, i.e. CT and PET images, usually come from different imaging equipments, both of them are produced from the same organ of the same patient. So when the spatial positions of two images are strictly uniform, $MI(I_R,I_F)$ reaches its peak value.

Studholme(Studholme C et al., 1999) found that the value of mutual information has some relevance which is subject to the overlap degree of two images to be matched. According to Studholme(Studholme C et al., 1999), in order to eliminate the effect resulted from the relevance, the mutual information is standardized as Eq.(4). The results of experiments show that it is more robust than Eq.(3).

$$MI(I_R,I_F) = \frac{H(I_R) + H(I_F)}{H(I_R,I_F)} \qquad (4)$$

4.3 Automatic matching of feature points
4.3.1 Automatic matching of feature point

The imaging principle of CT image tells that it reflects the detailed information about anatomical structure, while PET image denotes the functional information. Because the resolution of CT is higher than that of PET image, in order to realize the registration of two modals images, the PET image should be deformed to match the CT image, thus the CT image is defined as reference image, and the PET image is taken as floating image.

The main work for automatic fine registration by the FFD based on hierarchical B-splines is to find out some suitable feature points, which contain the points of ROI and the internal distribution points. For example, for the thorax, the thorax-wall is regarded as a rigid body due to its little deformation, while other organs in thorax such as heart and lung are always in the state of motion, so they are taken as non-rigid bodies. For current PET/CT scanning, the CT and PET scanning are carried out in sequence actually, not in the same time, in addition, the time for PET scanning is much longer than that of CT, thus it may lead to the difference of shapes from the PET and CT images in the same layer. For the thorax-wall is a rigid body, thus, the points on contour lines of thorax are taken as the feature points, while organs such as heart and lung, are always in motion, so internal distribution points can be randomly selected as feature points. On the other side, how to match the brighter ROI(region of interesting) of PET image with the corresponding ROI of CT image is an important task in multimodal medical image registration.

So, the operation of automatic matching of feature points is as follows, which is shown as Fig.3. ① Step 1. Shown as Fig.3(a), first the ROI with larger SUV, such as the pixel "F" of Fig.3(a), is selected from PET images by using the C-V level sets algorithm; then the corresponding feature points, such as the corresponding feature point "F' " of "F', are searched from CT images by using the mutual information as similarity measure. ② Step 2. Shown as Fig.3(b), the ROI, such the point "B", should be first extracted from the CT images, this can be done by using the C-V level sets algorithm. Then the corresponding feature points on the PET image, such the corresponding feature point "B' " of "B", are searched by employing the maximum mutual information algorithm. ③ Step 3. Shown as Fig.3(c), internal distribution points are randomly selected on the internal edge. And all of the feature points are matched automatically which is based on parallel computing method. Thus automatic matching of the initial feature points are realized, and the local deformation adjustment will be done according to the follow-up gradient descent coefficients correction.
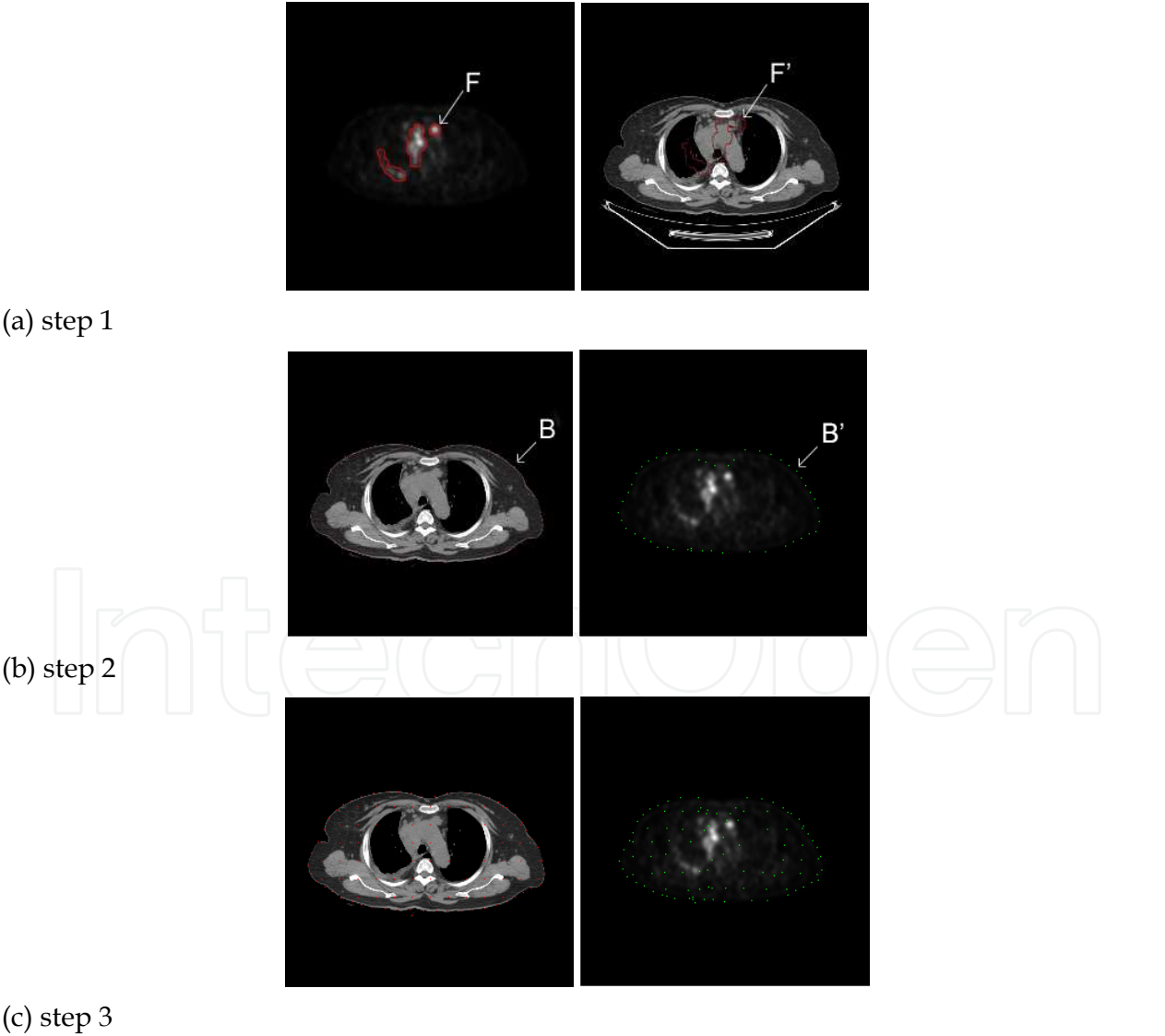

(a) step 1

(b) step 2

(c) step 3

Fig. 3. Illustration of automatic matching of feature points

4.3.2 ROI extraction based on improved C-V level sets method

Traditional Snake active contour modal shows some weaknesses: 1) the contour generated by initialization usually should be very near the real boundary, otherwise it will result in erroneous results; 2) the active contour is difficult to enter into concave domain.

Chan and Vese presented the C-V level set method based on optimal technique of curve evolution(Chan T F et al., 2001), simple Mumford-Shad Function, in which the image segmentation problem is connected with the optimization of Mumford-Shad Function, so that the efficiency and robustness of image segmentation are improved.

In this chapter, ROI, including the organ contour and the focus region, is extracted by the improved C-V level set method. The improved C-V level set method is based on a region-based active contour model, which avoids expensive re-initialization of the evolving level set function.

The partial differential equations(PDE) defined by level set function ϕ is:

$$\frac{\partial \phi}{\partial t} = \delta_\varepsilon(\phi)[\mu \operatorname{div}(\frac{\nabla \phi}{|\nabla \phi|}) - \nu - \lambda_1(I_0 - c_1)^2 + \lambda_2(I_0 - c_2)^2] = 0 \qquad (5)$$

where, $\delta_\varepsilon(\phi)$ is slightly regularized versions of *Dirac* measure $\delta(\phi)$; $\mu, \nu, \lambda_1, \lambda_2$ represents the weight of the corresponding energy term, respectively; I_0 is the object region; c_1, c_2 is the average intensity value inside and outside contour.

The procedure for ROI extraction using the improved C-V level set method are as follows:

1. Initialize level set function ϕ_n by ϕ_0, $n = 0$.
2. The initial curve is set, and the SDF(signed distance function) is also set according to the shortest distance between the point and curve, in which the value of SDF is positive inside curve, yet negative outside curve.
3. Compute $c_1 = \dfrac{\int_\Omega I_0 H_\varepsilon(\phi) dxdy}{\int_\Omega H_\varepsilon(\phi) dxdy}$, and $c_2 = \dfrac{\int_\Omega I_0(1 - H_\varepsilon(\phi)) dxdy}{\int_\Omega (1 - H_\varepsilon(\phi)) dxdy}$.
4. Solve the PDE in level set function ϕ iteratively. The iterative ϕ^{n+1} is computed by putting the global and local region value into Eq.(5).
5. Check whether the solution is stationary. If not, $n = n + 1$ and repeat.

4.3.3 Auto-matching method of feature points based on parallel computing

It is well known that the process of feature-points matching accounts for the most runtime of all the registration process, that is, the feature-point-matching process is the main factor which influences the efficiency of non-rigid registration process.

Feature points are signed in CT image, then their corresponding feature points are found from PET image. The matching process of feature points, which uses local searching strategy as said in section 4.3.1, will cost much time. In the matching process of feature points, the step of searching and matching of each feature point is independent, so the matching of feature points is processed by the method of parallel computing. Parallel computing can potentially further increase matching efficiency, in order to implement efficiently the registration of multi-model medical images data, the parallel matching technique based on high performance computation is used in this chapter. The cluster computing system is very

inexpensive and powerful for high-performance computing. It interconnects general-propose computers, such as workstation and PC, together to form a powerful computing platform through the rapid ethernet and the message-passing project, such as MPI(Message-Passing Interface) /PVM(Parallel Virtual Machine). In this chapter, the cluster computing system is designed to perform with MPI high performance computation-parallel image matching algorithm.

The parallel task partition strategies are a tradeoff between the communication cost and load balancing[13]. Here, the task partition could be implemented by domain decomposition. The followings are the steps of the parallel algorithm:

1. The management process broadcasts all of the data, including CT-PET image data and position of feature points in CT, to be processed to all the processes of the communication domain.
2. Each process computes the assigned start number, end number and amount of the processed feature points according to the process index.
3. The assigned feature points are matched independently in each process in turn, which is according to section 4.3.1.
4. The result is sent to the management process. And the management process receives and saves all the result.

4.4 Global rigid deformation based on principal axes algorithm

The global rough registration for rigid deformation is realized by adopting principal axes algorithm(Louis K A et al., 1995) in this chapter. First, the corresponding feature points of PET and CT images are searched by using the method presented in section 4.3, respectively. And then the centroids of two image contours are calculated, and the centroid of PET image couture is adjusted to adapt to that of CT image.

4.5 Local fine registration based B-splines adaptive FFD

When only considering local information for image registration, image deformation will be resulted, in the mean time, if elastic deformation is directly employed for image registration, it may result in mismatch. So the local elastic deformation is realized by applying the adaptive FFD based on hierarchical B-splines method. The flow chart is shown as Fig.4.

4.5.1 Registration based on B-splines FFD method

The principle of the FFD method(Huang Xiaolei et al., 2006) is that the object shape is changed and controlled through controlling the control points of control framework. The control framework and a group of basis functions constitute an entity which are some Bernstein polynomials. For B-spline only affects local deformation, so, when some of the feature points of a two-dimensional image are moved only the vicinal points are affected, not all the points in the image are deformed, so cubic B-splines tensor product of two variables is adopted as the FFD deformation function.

Let Π be a two-dimension image in $x - y$ plane. Suppose $p = (u, v)$ is a point on image Π, where $1 \le u \le m$, $1 \le v \le n$. When some deformation of image Π is generated , its shape can be represented by a vector function $h(p) = (x(p), y(p))$. Let Ψ is a control point grid of $(m+3) \times (n+3)$ covering on Π. Suppose ψ_{IJ} expresses the position coordinate (I, J) in Ψ. Shape function h can be represented by ψ_{IJ} which is shown in Fig.5.

$$h(u,v) = \sum_{k=0}^{3} \sum_{l=0}^{3} B_k(s)B_l(t)\psi_{(I+k)(J+l)} \tag{6}$$

Where,

$$I = \left\lfloor \frac{u}{m+2} \right\rfloor - 1 \,, J = \left\lfloor \frac{v}{n+2} \right\rfloor - 1 \,, s = \frac{u}{m+2} - \left\lfloor \frac{u}{m+2} \right\rfloor \,, t = \frac{v}{n+2} - \left\lfloor \frac{v}{n+2} \right\rfloor .$$

$B_k(s)$ and $B_l(t)$ are the uniform cubic B-spline basis function of vectors s and t, respectively. For $B_l(t)$ it can be described as follows:

$$\begin{aligned}
B_0(t) &= (-t^3 + 3t^2 - 3t + 1)/6 \\
B_1(t) &= (3t^3 + 6t^2 + 4)/6 \\
B_2(t) &= (-3t^3 + 3t^2 + 3t + 1)/6 \\
B_3(t) &= t^3/6
\end{aligned} \tag{7}$$

where $0 \le t \le 1$.
The expression for $B_k(s)$ is the same as for $B_l(t)$.
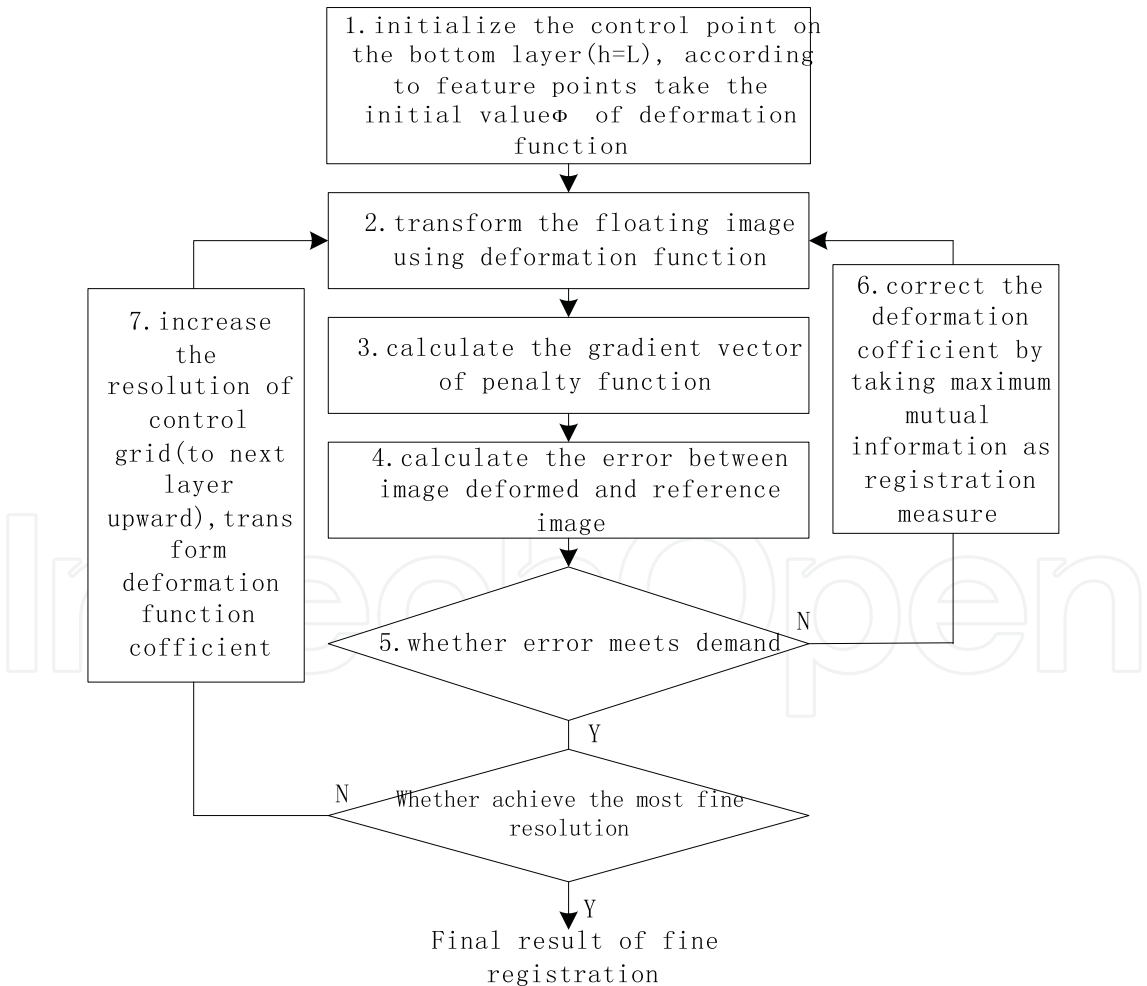
Fig. 4. Local fine registration using a free-form deformation(FFD) based on hierarchical B-splines
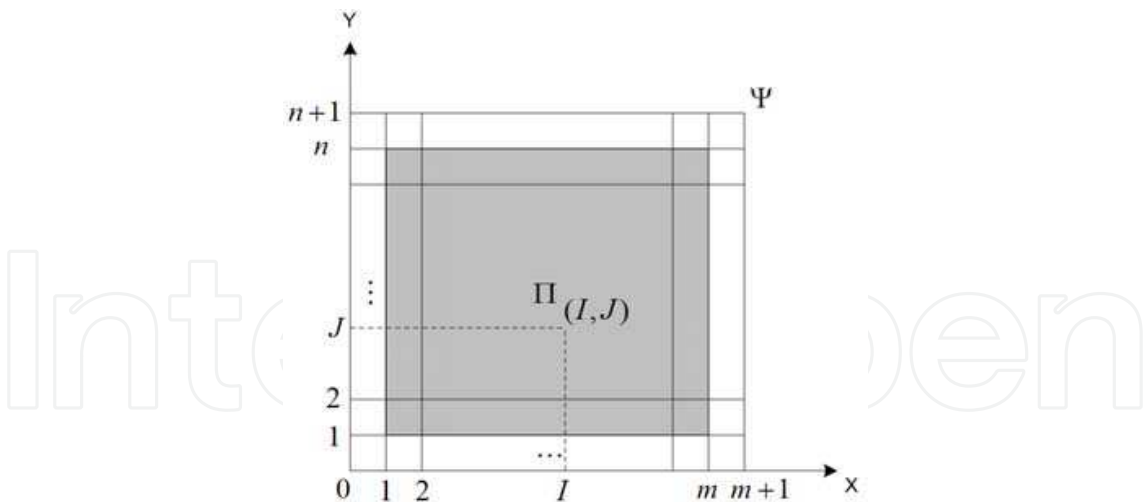
Fig. 5. Initial position of original image and control point lattice

4.5.2 Reverse mapping - elimination of the hole phenomenon

In the registration process, the image to be processed should be deformed to form a new image. In doing so, there are two kinds of methods to be selected: forward mapping and reverse mapping. For forward mapping, it is required that every pixel from input image should be mapped to output image through transformation function, which is difficult to guarantee that all the points are mapped, i.e., sometimes, some points may be omitted. When such case happens, it is called hole phenomenon. On the contrary, the reverse mapping method can enable each pixel in output image to find its corresponding point in input image, in doing so, there is no hole phenomenon to happen. In this chapter, the registration function is established based on the feature points of floating image, each pixel of the image to be matched is input to the registration transformation function, then the corresponding position of the reference image is obtained. Thus it can eliminate hole phenomenon.

4.5.3 Fine registration of multimodal medical image

For the position, size and shape of internal organs and tissues are affected by involuntary physiological movements or motions of patient, this will lead to elastic deformation in the local position of organs. However, due to the local deformation of medical image based on local information, so it is easy to result in mismatch if executing elastic deformation directly. To solve such problem, B-spline function can be selected to generates a smooth curve(or smooth plane) to approximate the control point. By comprehensively considering the accuracy of fitting function, the deformation smoothness, the calculation complexity and registration accuracy, an automatic fine registration of multimodal medical images based on hierarchical B-splines adaptive FFD is presented in this chapter. Flow chart is shown as Fig.4.

4.5.4 Implementation of fast FFD registration

In the registration process, the image to be processed should be deformed to form a new image. In doing so, there are two kinds of methods to be selected: forward mapping and reverse mapping. For forward mapping, it is required that every pixel from input image should be mapped to output image through transformation function, which is difficult to

guarantee that all the points are mapped, i.e., sometimes, some points may be omitted. When such case happens, it is called hole phenomenon. On the contrary, the reverse mapping method can enable each pixel in output image to find its corresponding point in input image, in doing so, there is no hole phenomenon to happen. In this chapter, the registration function is established based on the feature points of floating image, each pixel of the image to be matched is input to the registration transformation function, then the corresponding position of the reference image is obtained. Thus it can eliminate hole phenomenon.It is well known that medical image registration is a very time-consuming task, which limits the clinical applications of such method to some degree. In order to overcome such shortcoming, some optimization measures can be taken to improve it. On this aim, a new registration method combining the FFD algorithm and maximum mutual information is presented, in which the optimization problem can be regarded as a nonlinear programming problem. This chapter adopts gradient descent method to implement fast FFD local fine registration, in which step adjusting is adapted based on maximization of mutual information.

The mutual information is taken as the cost function for the presented medical image registration method, then a global optimal solution is $\Theta^* = \arg\min_{\Theta} C(\Theta)$. In this research, the gradient descent method is used to solve the extreme value of coefficient matrix Θ. Although only the local extrema can be obtained by using the presented method, whose operation speed is much faster than the traditional ones, and due to the smoothness constraint, this method can overcome the problem of local extrema effectively in calculation process of deformation field.

The calculation process for this method is already described in Fig 3. Here some additional explanations are given as follows:

1. Gradient computation

   The gradient of cost function C is shown as follows:

$$\nabla C = \frac{\partial C(\Theta, \Phi^l)}{\partial \Phi^l} \tag{8}$$

   where Φ^l is the control grid coordinate of the l-th layer, Θ is deformation coefficient. Here, the maximum mutual information entropy is taken as the cost function C, and its gradient at the point (u, v) is a vector that can be simplified as:

$$\nabla C = |f(u,v) - f(u-1,v)| + |f(u,v) - f(u,v-1)| \tag{9}$$

2. Correction of deformation coefficient

   In the algorithm, the maximum mutual information entropy is taken as registration measure to test whether the pre-set error is achieved or not. If not achieved, the deformation coefficients should be corrected. The iterative algorithm for control points is shown as follows:

$$\Phi_i^{(t+1)} = \Phi_i^{(t)} - \mu \frac{\nabla C}{||C_i||} \tag{10}$$

   where $i \in I_C$, I_C is the grid spatial image after deformation, t is iterative number, μ is iterative step.

5. Fusion of multimodal medical image

5.1 Image fusion based on wavelet transform

After the registration of CT and PET images, their sequence images are fused by applying a image fusion method based on parallel computing and wavelet transform with the fusion rule of combining the local standard deviation and energy. The followings are the steps of the fusion algorithm:

Step 1. The CT and PET images are encoded by a 3-level wavelet decomposition with Daubechies 9/7 biorthogonal wavelet filter banks.

Step 2. Compute the average value of wavelet coefficients $D_{CT}(i,j)$ / $D_{PET}(i,j)$ of the CT and PET images.

$$\begin{cases} D_X(i,j) = \sum_{s \in S, t \in T} \omega(s,t) D_X(i+s, j+t, k, l) \\ X = CT, PET \end{cases} \tag{11}$$

Where (i, j) denotes the position of the center of the current window; k denotes the level of wavelet decomposition ($k = 1,2,3$); l denotes frequency band; (s, t) denotes the position in the current window; $\omega(s, t)$ denotes the weight of the coefficient in (s, t), and the further away from the center it is, the less the weight becomes; $\sum_{s \in S, t \in T} \omega(s,t) = 1$, where S and T denote the norm of the current window.

Step 3. CT and PET images are fused based on wavelet transform by employing fusion rule of combining the local standard deviation and energy.

In clinic application, physicians are interested in the position signs of the tumor. The anatomical images depict clearly primarily morphology of human body through the abundant texture. Therefore, the selected activity measure should reflect the texture pattern of the image. Each pixel value in a smooth region of a image is nearly equal, yet it changes severely in a rough region. So the local standard deviation is regarded as the activity measure of coefficients. Furthermore, the local energy reflects the absolute intensity of the signal change, and the large absolute intensity of the signal change reflect the obvious feature of the image. So the image feature is described in uniform by the local standard, which reflects the definition. Therefore, the local standard deviation and energy standard are selected as the activity measure of the coefficients.

① Let A_X denote the activity measure based on local standard deviation.

$$A_X(i,j) = \sqrt{\sum_{s \in S, t \in T} \omega(s,t) \left[D_X(i+s, j+t, k, l) - D_X(i,j) \right]^2} \tag{12}$$

Let δ_{CT} and δ_{PET} denote the weight that the activity measure based on local standard deviation assigned to CT and PET, respectively.

$$\begin{cases} \delta_{CT} = \dfrac{\left[A_{CT}(i,j)\right]^{\alpha}}{\left[A_{CT}(i,j)\right]^{\alpha} + \left[A_{PET}(i,j)\right]^{\alpha}} \\[4mm] \delta_{PET} = \dfrac{\left[A_{PET}(x,y)\right]^{\alpha}}{\left[A_{CT}(i,j)\right]^{\alpha} + \left[A_{PET}(i,j)\right]^{\alpha}} \end{cases} \tag{13}$$

Where α is a adjustable parameter. When $\alpha > 0$, the higher activity measure is, the more it weights. Here, let α equal to 1.8。

②Let B_X denote the activity measure based on local energy.

$$B_X(i,j) = \sum_{s \in S, t \in T} \omega(s,t) D_X^2(i+s, j+t, k, l) \tag{14}$$

Let δ_{CT} and δ_{PET} denote the weight that the activity measure based on local energy assigned to CT and PET, respectively.

$$\begin{cases} \varepsilon_{CT} = \dfrac{B_{CT}(i,j)}{B_{CT}(i,j) + B_{PET}(i,j)} \\[4mm] \varepsilon_{PET} = \dfrac{B_{PET}(i,j)}{B_{CT}(i,j) + B_{PET}(i,j)} \end{cases} \tag{15}$$

③After combining the local standard deviation and energy, wavelet coefficients of fused image D_F is

$$\begin{aligned} D_F(i,j) &= \left[\delta_{CT} D_{CT}(i,j) + \delta_{PET} D_{PET}(i,j)\right] \times \lambda \\ &+ \left[\varepsilon_{CT} D_{CT}(i,j) + \varepsilon_{PET} D_{PET}(i,j)\right] \times \mu \end{aligned} \tag{16}$$

Where, λ, μ are adjustable parameters, $\lambda + \mu = 1$. The image intensity gets stronger as μ increases; and the edge of intensity get sharper as λ increases, thus the blur of the edge is avoided as possible as we can if λ / μ is adjusted suitably.

Step 4. The approximate coefficients C_J^{CT} and C_J^{PET} through wavelet transform of CT and PET image are processed. $\hat{C}_J^F$ is computed by formula 21:

$$\hat{C}_J^F = (C_J^{CT} + C_J^{PET}) / 2 \tag{17}$$

Step 5. The fused image F is gotten by wavelet inverse transform using all of the wavelet coefficients D_F and the approximate coefficients.

and saves all the result.

5.2 Parallel image fusion
5.2.1 Necessity of parallel image fusion
In image fusion, it becomes more computationally expensive as the image data and its level of wavelet decomposition increase. Because parallel computing can potentially further

increase fusion efficiency, the parallel image fusion technique based on high performance computation is used in this chapter. As said in section 4.3.3, the cluster computing system is very inexpensive and powerful for high-performance computing. In order to implement effectively and efficiently the fusion of mass multimodal medical images data, a parallel multimodal medical image fusion method based on wavelet transform is presented. In this chapter, the cluster computing system is designed to perform with MPI high performance computation-parallel image fusion algorithm based on wavelet transform.

5.2.2 Implement of parallel image fusion based on wavelet transform

In image fusion, it becomes more computationally expensive as the image data and its level of wavelet decomposition increase. Because parallel computing can potentially further increase fusion efficiency, the parallel image fusion technique based on high performance computation is used in this chapter. As said in section 4.3.3, the cluster computing system is very inexpensive and powerful for high-performance computing. In order to implement effectively and efficiently the fusion of mass multimodal medical images data, a parallel multimodal medical image fusion method based on wavelet transform is presented. In this chapter, the cluster computing system is designed to perform with MPI high performance computation-parallel image fusion algorithm based on wavelet transform.

Partitioning divides the problem into parts, which is the basis of all parallel programming. Partitioning can be applied to the programming data. This is called data partitioning or domain decomposition. The parallel task partition strategies are a tradeoff between the communication cost and load balancing. When an image is encoded or decoded by a M-level wavelet transform or inverse decomposition, the processed wavelet coefficients of each level are the input of the next level, so the processions between two adjacent levels are of strong correlation. But it is of high parallelism for each level to implement 1D wavelet transform/inverse decomposition row by row or column by column. Moreover, the result after implementing 1D wavelet transform/inverse decomposition is used for the next level wavelet transform. So when the sub-image is encoded by wavelet transform, the task partition could be implemented by domain decomposition. The followings are the steps of the parallel algorithm:

1.   The management process broadcasts all of the data to be processed to all the processes of the communication domain.
2.   The assigned rows of data are encoded/decoded by 1D wavelet transform/inverse decomposition in each of the processes, then the result is sent to the management process.
3.   The management process broadcasts all of the data processed to all of the processes of communication domain.
4.   The assigned columns of data are encoded/decoded by 1D wavelet transform/inverse decomposition in each of the processes, then the result is sent to the management process.
5.   Repeat step 1-4, until M-level wavelet transform/inverse decomposition is finished.

From the above steps, a conclusion could be drawn that there are several times of data communication in each of M-level wavelet transform/inverse decomposition, so that the parallel efficiency is very low because the communication cost is relatively expensive, especially for the image data in miniature. Therefore, in parallel image fusion of medical sequence images, domain decomposition is applied. All the processes are processed in parallel, however in each process images are fused sequentially.

Multimodal medical sequence images are fused in 3D CRTP. The steps of the algorithm of parallel image fusion of medical sequence images are illustrated in Fig.6.
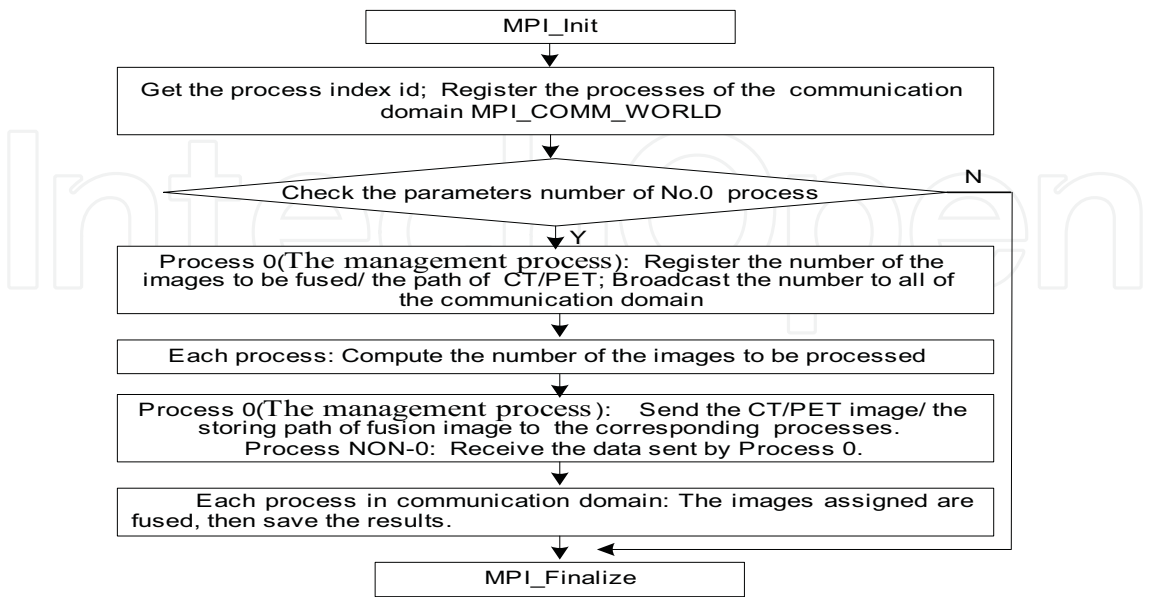

Fig. 6. The flowchart of parallel sequence images fusion

6. Experimental results in 3D conformal radiotherapy treatment planning

In this chapter, a cluster computing system is developed, whose configurations consist of: ①Operation system: Windows Server 2003; ②Network card: 100M b/s Realtek RTL8139 Family PCI Fast Ethernet NIC; ③Parallel software package: MPICH 2-1.0.5p2-win32; ④ Node configurations: processor Intel Pentium 4, CPU 3.0GHz/ 1.00GB RAM; display card, NVIDIA Quadro FX 1400. ⑤ compiler: Visual C++6.0, the programming language is C++.

6.1 Effect evaluation for medical image registration and fusion
6.1.1 Effect evaluation for registration method

The presented image registration method applying adaptive FFD which is based on hierarchical B-splines algorithm is shown as Fig.2.The original images CT(512×512) and PET(128×128), which come from the thorax image sequences, are shown as Figs 7 and 8, respectively. Fig.9 is the processing result of feature points based on parallel computing and ROI extraction by applying the C-V level sets method. The edge curve in Fig.9(a) is the result by applying the edge extraction method of C-V level sets, the regular points in the middle are the selected feature points with 8 interval pixels; the points of Fig.9(b) are the corresponding feature points of Fig.9(a). Fig.10 is the global rough registration result using the principle axes algorithm. Fig.11 is the result of local fine registration of Fig.10 by adopting the presented registration algorithm based on hierarchical B-splines adaptive FFD. Fig.12 shows the data field change pre and post registration.

The effective evaluation for registration method, especially for multimodal medical image is always very difficult. Due to multi-images to be matched are obtained at different time or under different conditions, it is difficult to find a common standardized criteria for the evaluation of the registration method. Usually the following factors are chosen to evaluate

the image registration method, for example, registration speed, robustness, registration precision, etc.. For medical image registration, the registration effect should be first considered. The common evaluation methods mainly are phantom, criteria and visual method.
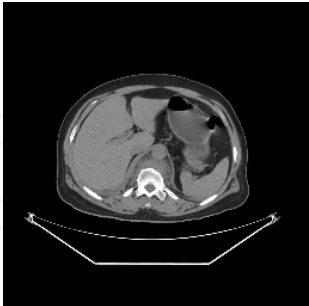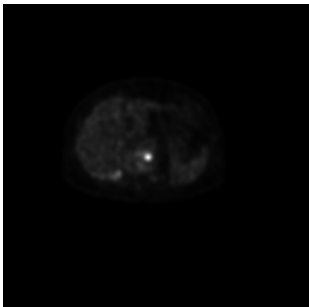

Fig. 7. CT image(reference image)

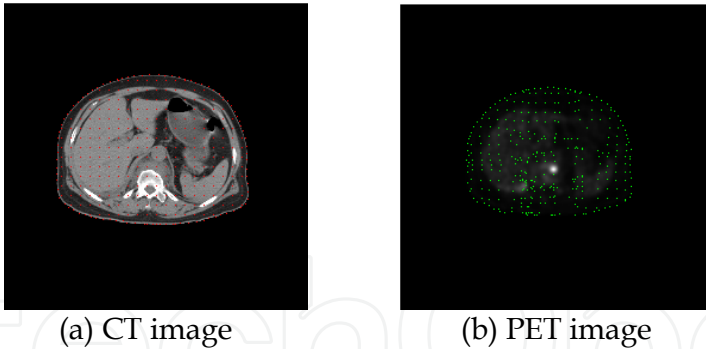Fig. 8. PET image(floating image)

(a) CT image   (b) PET image

Fig. 9. Feature points matched based on parallel computing and ROI extraction by the C-V level sets method
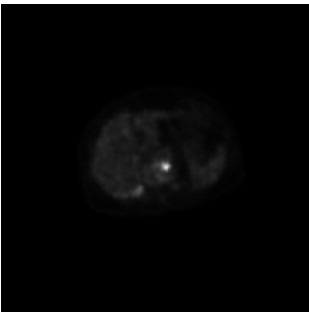
Fig. 10. Global coarse registration by PAA
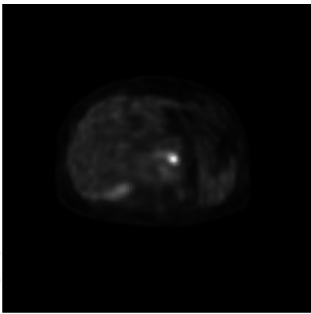
Fig. 11. Local fine registration image by FFD based on hierarchical B-splines method
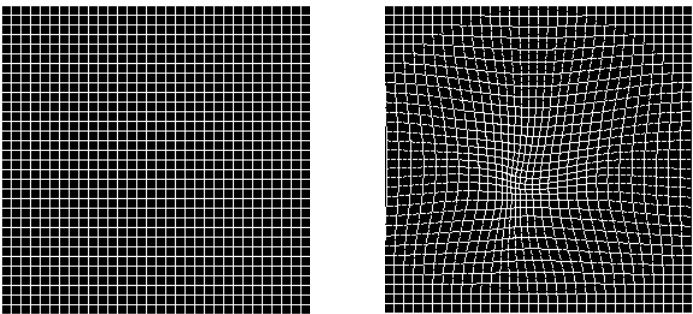
(a) Original data set   (b) data set after transformation

Fig. 12. Data set change pre and post registration

The quantitative evaluation method based on image statistical characteristics is adopted in this chapter. including Maximum Information entropy(MI), Root Mean Square error(RMS error), Correlation Coefficient(CC). They can give a quantitative assessment index for registration algorithm. Generally speaking, the statistical characteristic method is currently an objective and practical evaluation method.

Suppose there are two images I_1, I_2, the size of image is $M \times N$, then the RMS is defined as follows:

$$RMS = \sqrt{\frac{\sum\limits_{i=0}^{M-1}\sum\limits_{j=0}^{N-1}\left(I_1(i,j) - I_2(i,j)\right)^2}{M \times N}} \tag{18}$$

If the RMS value becomes smaller, it indicates the difference between two images is small, it proves the registration effect is better. Here, the statistical characteristic CC is employed as the evaluation criteria: for registration effect

$$CC = \frac{\sum\limits_{i=0}^{M-1}\sum\limits_{j=0}^{N-1}\left(I_2(i,j) - \overline{I_2}\right)\left(I_1(i,j) - \overline{I_1}\right)}{\sqrt{\sum\limits_{i=0}^{M-1}\sum\limits_{j=0}^{N-1}\left(I_2(i,j) - \overline{I_2}\right)^2}\sqrt{\sum\limits_{i=0}^{M-1}\sum\limits_{j=0}^{N-1}\left(I_1(i,j) - \overline{I_1}\right)^2}} \tag{19}$$

where, $\overline{I_1}$ and $\overline{I_2}$ are the average gray values of two images: $\overline{I_1} = \dfrac{\sum\limits_{i=0}^{M-1}\sum\limits_{j=0}^{N-1} I_1(i,j)}{M \times N}$,

$\overline{I_2} = \dfrac{\sum\limits_{i=0}^{M-1}\sum\limits_{j=0}^{N-1} I_2(i,j)}{M \times N}$. The CC value ranges from 0 to 1, when there is no any correlation between two images, the value is 0; vice versa, if two images are completely matched, CC tends to 1, meaning a very ideal situation. As a matter of fact,, the value of CC often is very small, especially for multimodal medical image registration.

The quantitative evaluation results for each registration method are shown in Table.1. The MI, RMS, and CC are used to evaluate each registration method, by analyzing the qualitative indexes for each method, it can be concluded that the presented registration algorithm is better than other traditional methods.

Registration method	MI	CC	RMS
Before registration	0.308430	0.648445	51.824407
Maximum mutual information	0.315437	0.671658	51.760785
Principle axes algorithm	0.280123	0.634221	52.125753
Multi-level B-splines	0.342456	0.692275	50.753875
The proposed mehtod (principle axes algorithm + H B-splines)	0.372521	0.701248	50.554238

Table 1. Comparisons among different registration methods

6.1.2 Effect evaluation for fusion method

In the experiment, CT slices(512*512*267) and PET(128*128*267) are from a male lung-cancer person. CT and PET sequence images are fused by applying the presented parallel multimodal medical image fusion method based on wavelet transform with fusion rule of combining the local standard deviation and energy. Results are shown as Fig.13, in which Fig.13(a) is No.183 CT slice of sequence images, Fig.13(b) is No.183 PET slice, Fig.13(c) is the corresponding matched result of Fig.13(a) and Fig.13(b) by using the presented registration method, and Fig.13(d) is the corresponding fusion image of them. There is some nodular shadows in basel segment of the lower lobe of left lung by viewing the CT slice. And there is a bright spot in the middle of the PET slice, which displays a high absorption region of imaging radiopharmaceuticals, yet the morphology of the cancer region is not very clear. The fusion image depict clearly the corresponding relation between the region of nodular shadows in CT slice and the region of cancer permeability in PET slice. Experimental results demonstrate that the edge and texture features of the multimodal images are reserved effectively by the presented fusion method based on wavelet transform with the fusion rule of combining the local standard deviation and energy. Therefore, the relative position between the tumor and its adjacent tissues could be obtained easily through analyzing the medical data sets which are fused the information of functional mages and anatomical images.
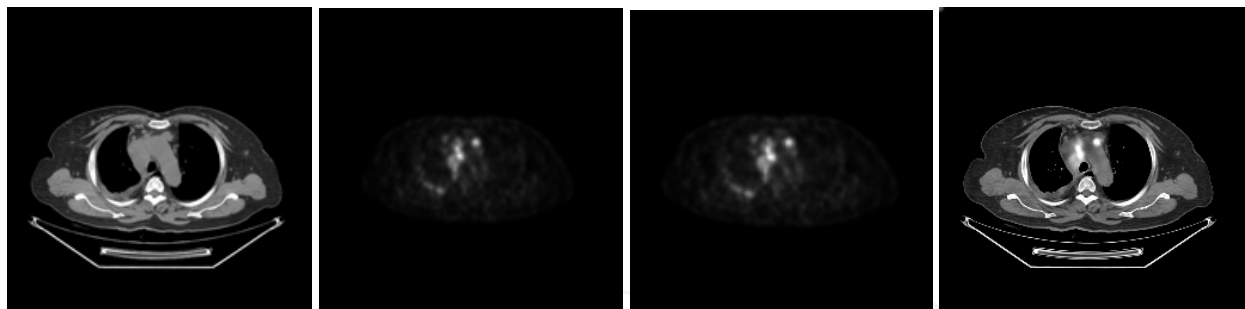
(a)Original CT image   (b)Original PET image   (c)Matched image   (d) Fusion image

Fig. 13. Chest CT and PET image fusion

6.1.1 Effect evaluation for registration method

Generally, fusion image evaluation criteria includes the subjective evaluation and objective evaluation. The objective valuation method is used in this chapter. Various statistical characteristics of the image are used, such as mean, standard deviation, entropy and cross-entropy.

1. Standard deviation (SD) Gray variance reflects the extent of deviation from the mean of the gray value. The greater the standard deviation is, the more dispersed the distribution of gray levels is.

2. Information entropy (IE) Information entropy reflects the average amount of information that the fusion image contains. The larger the entropy is, the more information the image carries. The image's information entropy E is defined:

$$E = -\sum_{i=0}^{Z} P_i \log_2 P_i \tag{20}$$

Where Z is the maximum gray level, P_i is the probability of i gray level.

3. Joint entropy (JE) The larger the joint entropy between fusion image and original image is, the more information the fusion image contains. The joint entropy between fusion image F and original image A is defined as follows.

$$UE_{FA} = -\sum_{i=0}^{Z_F}\sum_{j=0}^{Z_A} P_{FA}(i,j)\log_2 P_{FA}(i,j) \tag{21}$$

Where, P_{FA} represents the joint probability density of two images.

In this experiment, the fusion results are evaluated by applying the above methods. Experiments show that the evaluation indexes of this presented method are superior to other fusion methods, the evaluation indexes of each method are shown in Table 2.

6.2 Efficiency comparison
6.2.1 Efficiency comparison for registration method

In this chapter, multimodal medical image registration is adapted based on adaptive free-form deformation and gradient descent. Moreover, the feature points are matched based on parallel computing. So, comparing to the traditional methods, the efficiency of the presented registration method has been greatly improved.

	SD	IE	JE (CT)	JE(PET)
weighted mean	328.545	4.691806	6.143996	5.620486
maximum	385.560	4.830680	8.370359	5.902740
local energy	162.497	5.052476	8.376337	6.134338
local standard deviation	415.144	5.810895	7.730113	6.800253
The presented method	383.129	5.987878	8.423761	6.997364

Table 2. Quantitative evaluation of fusion image

1. Efficiency of registration process of based on adaptive free-form deformation and gradient descent

As shown in Fig.14(a) and Fig.14(b), the average number of cycling for the presented method is about 3.12, and the registration position is searched only using about 84.24 steps. While the number of cycling for the traditional method is about 50 to 60 and more than 300 steps for searching, much larger than the presented algorithm. It demonstrates that the presented registration method is more efficient, and its searching speed is much faster than traditional algorithm.

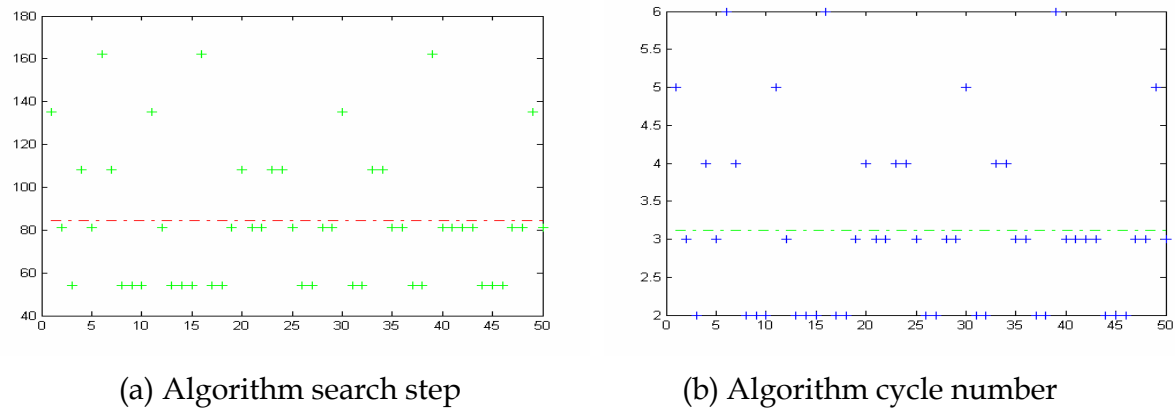(a) Algorithm search step   (b) Algorithm cycle number

Fig. 14. Efficiency of the presented algorithm based on Gradient Descent

2. Efficiency of feature-points matching based on parallel computing

In the experiment, 3 pairs CT-PET images, in which CT resolution is 512*512 and PET resolution is 128*128, are from a male lung-cancer person.

The runtime of feature-points matching based on parallel computing in the cluster computing system is shown in Fig.15.The runtime of all the registration process based serial computing is 335 seconds. The runtime of the process of feature-points matching based on serial computing is 170 seconds, and the runtime of finding the corresponding feature points of CT image from PET image is 156.5 seconds, which accounts for 92% of all the feature-points-matching process. The runtime of feature-points matching based on parallel computing using 5 processors is 32 seconds, and all the registration process costs 43 seconds. It is obvious that the runtime of registration decreases obviously. Moreover, the parallel system efficiency keeps about 0.97, thus the algorithm is of good expansibility so that the runtime will decrease more if more processors is used. It is obvious that the runtime of registration decreases obviously.

So, comparing to the traditional methods, the efficiency of the presented registration method has been greatly improved. Because, on one hand, the presented multimodal medical image registration is adapted based on adaptive FFD and gradient descent; on other hand, the feature points are matched efficiently based on parallel computing.
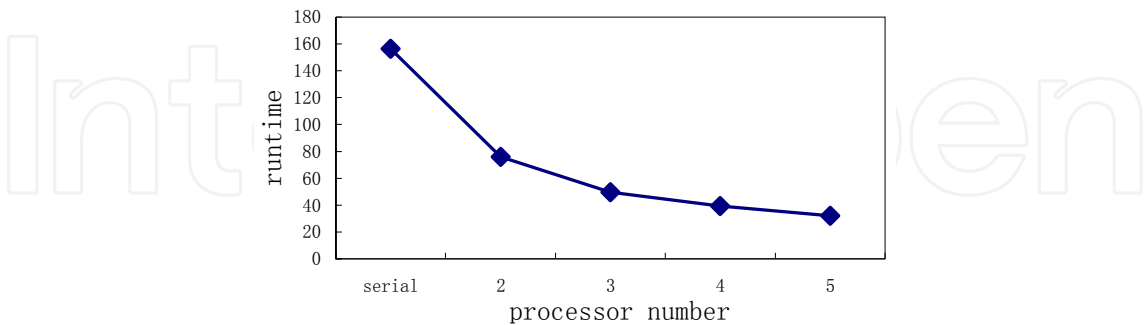

Fig. 15. Efficiency of the feature-point matching based on parallel computing

6.2.2 Efficiency comparison for fusion method

In order to evaluate the performance of parallel computing, two parameters must be introduced: the speedup factor $S(p)$ and parallel efficiency E (Yasuhiro K. et al., 2004).

$$S(p) = ts / tp \tag{22}$$

Where $S(p)$ is a measure of relative performance; p is the number of processors; tp is the execution time for solving the same problem on a multiprocessor; ts is the execution time of the best sequential algorithm running on a single processor.

It is sometimes useful to know how long processors are being used on the computation, which can be found from the system efficiency. The efficiency, E, is defined as

$$E = S(p) / p \tag{23}$$

The comparison of run time is shown in Table 3. It is obvious that the runtime of parallel sequence images fusion decreases obviously. From Table 3, the runtime of sequences image(267 images) fusion is only 43.773 seconds if using parallel computation of 6 processors, which is far less than that of sequential algorithm. Moreover, the parallel system efficiency keeps about 0.97, thus the algorithm is of good expansibility so that the runtime will decrease more if more processors is used. So it can be concluded that the calculation time is fast enough for clinical use.

	sequential algorithm	Parallel algorithm			
		processor 1	processors 2	processors 4	processors 6
runtime	251.468s	259.757s	130.103s	65.090s	43.773s
$S(p)$	─ ─	0.97	1.93	3.86	5.74
E	─ ─	0.97	0.97	0.97	0.96

Table 3. Time performance of parallel sequences image fusion(267 images)

6.3 Experiment results in 3D Conformal Radiotherapy Treatment Planning

The experiment results in 3D CRTPS are shown as Fig.16. Fig.16 is the interface of 3D Conformal Radiotherapy Treatment Planning System(3D CRTPS) which is developed by ourselves. Fig.16(a) and 16(b) consist of four windows respectively: No.1 is the 3D volume rendering result; No.3 and No.4 are CT image(512*512) and PET image(128*128), respectively. These slices correspond to the position showed by white line in No.1 window; No.2 is the registration and fusion result of CT and PET. The technologist can give diagnosis by using the system.

         (a) Viewed from the front   (b) Viewed from the back
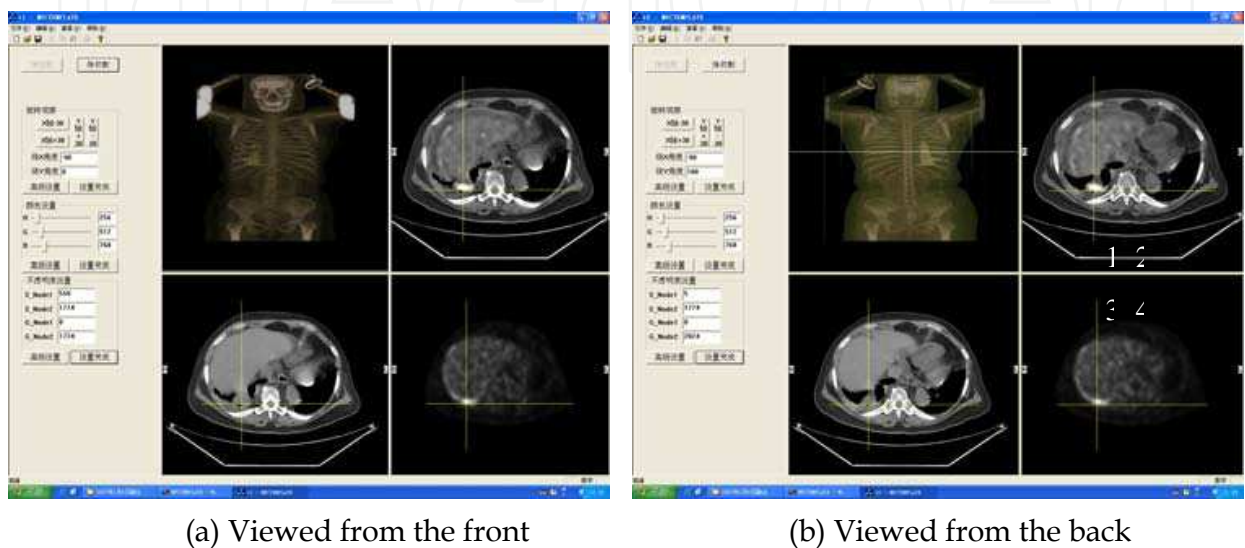
Fig. 16. Experimental result of cases

7. Discussions and conclusions

A rapid image registration and fusion method is presented in this chapter. This presented automatic registration method is based on parallel computing and hierarchical adaptive free-form deformation(FFD) algorithm. After the registration of multimodal images, their sequence images are fused by applying a image fusion method based on wavelet transform with the fusion rule of combining the local standard deviation and energy.

The results of the validation study indicate that the presented multimodal medical image registration and fusion method can improve effect and efficiency and meet the requirement of 3D conformal radiotherapy treatment planning. And the radiologists who validated the results felt the errors were generally within clinically acceptable ranges.

By analyzing the qualitative indexes, such as MI, RMS, and CC, for each method, it can be concluded that the presented registration algorithm is better than other traditional methods. And experiments show that the evaluation indexes(SD, IE, JE) of this presented method are superior to other fusion methods, such as the weighted mean method, the maximum method, the local energy method and the local standard deviation method.

In addition, comparing to the traditional methods, the efficiency of the presented registration and fusion method has been greatly improved, because in this chapter multimodal medical image registration is realized based on gradient descent, and the feature points are matched based on parallel computing. Moreover, image fusion is also carried out by parallel computing.

8. References

Aparna Kanakatte, Jayavardhana Gubbi, Nallasamy Mani, et al.(2007). A pilot study of automatic lung tumor segmentation from positron emission tomograph images using standard uptake values, *Proceedings of the 2007 IEEE Symposium on Computational Intelligence in Image and Signal Processing (CIISP 2007)*, pp. 363-368, ISBN:1-4244-0707-9, conference location: Honolulu, HI, USA, June, 2007, IEEE, Los Alamitos

Bardinet E, Cohen LD, Ayache N. (1996). Tracking and motion analysis of the ventricle with deformable superquadrics. *Medical Image Analysis*, Vol.1, No.2, 1996, 129-149, ISSN:1361-8415

Chan T F, Vese L A. (2001). Active contours without edges. *IEEE Transaction on Image Processing*, Vol.10, No.2, 2001, 266-277, ISSN:1057-7149

David M., David R.H. , et al. (2003). PET-CT image registration in the chest using free-form deformations. *IEEE Transaction on Medical Image*, Vol.22, No.1, 2003, 120-128, ISSN: 0278-0062

Huang Xiaolei, Paragios, N.; Metaxas, D.N.(2006). Shape registration in implicit spaces using information theory and free form deformations. *IEEE Transactions on Pattern Analysis and Machine Intelligence*, Vol.28, No.8, 2006, 1303- 1318, ISSN:0162-8828

Ino Fumihiko, Ooyama Kanrou, and Hagihara Kenichi.(2005). A data distributed parallel algorithm for nonrigid image registration. *Parallel Computing*, Vol..31, No.1, 2005, 19-43, ISSN:0167-8191

Josien P. W. Pluim, J. B., Antoine Maintz, and Max A. Viergever(2003). Mutual-information-based registration of medical images: A Survey. *IEEE Transaction on Medical Image*, Vol.22, No.8, 2003, 986-1004, ISSN: 0278-0062

Lee Seungyong, Wolberg George, and Shin Sung Yong. (1997). Scattered data interpolation with multilevel B-Splines. *IEEE Transactions on Visualization and Computer Graphics*, Vol.3, No.3, 1997, 228-244, ISSN:1077-2626.

Louis K A, Atam P D, Joseph P B.(1995). Three_dimensional anatomical model_based segmentation of MR brain images through principal axes registration. *IEEE transactions on biomedical engineering*, Vol.42, No.11, 1995, 1069-1077, ISSN: 0018-9294

Maintz J.B.A., Vigergever M.A. (1998). A survey of medical image registration. *Medical Image Analysis*, Vol.2, No.1, 1998, 1-36, ISSN:1361-8415

M. Betke, H. Hong, and J. P. Ko. (2003). Landmark detection in the chest and registration of lung surfaces with an application to nodule registration. *Medical Image Analysis*, No.7, 2003, 265-281, ISSN:1361-8415

Park J H, Kim K O, Yang Y K.(2001). Image Fusion Using Multiresolution Analysis, *IEEE Int'l Conf on Geoscience and Remote Sensing (IGARSS)*, pp. 864-866, ISBN:0-7803-7031-7, conference location: Sydney, NSW, Australia, 2001, IEEE, Los Alamitos

Ruechert D., Sonoda L.I., Hayes C., et al.(1999). Nonrigid registration using free-form deformations:application to breast MR images. *IEEE Transaction on Medical Image*, Vol.18, No.8, 1999, 712-721, ISSN: 0278-0062

S-C. Huang. (2000). Anatomy of SUV. Nuclear medicine and biology, Vol.27, No.7, 2000, 643-646, ISSN:0969-8051

S.K.Warfield, F.A.Jolesz, and R.Kikinis.(1998). A high performance computing approach to the registration of medical image data. *Parallel Computing,* Vol..24, 1998, 1345-1368, ISSN:0167-8191

Stefan Klein, Marius S., josien P.W.P. (2007). Evaluation of optimization methods for nonrigid medical image registration using mutual information and B-Splines. *IEEE Transaction on Image Processing,* Vol.16, No.12, 2007, 2879-2890, ISSN:1057-7149

Studholme C, Hill DLG, Hawkes DJ (1999). An overlap invariant entropy measure of 3D medical images alignment. *Pattern Recognition,* Vol.32,No.1, 1999, 71-86, ISSN:0031-3203

T. Blaffert && R. Wiemker. (2004). Comparison of different follow-up lung registration methods with and without segmentation, *SPIE*, vol. 5370, 2004, 1701-1708, ISSN:0277-786X

Yasuhiro K., Fumihiko I., Yasuharu M., et al.(2004). High-performance computing service over the internet for intraoperative image processing. *IEEE transactions on information technology in biomedicine,* Vol.8, No.1, 2004, 36-46, ISSN:1089-7771

Zhiyong Xie, Gerald E. Farin.(2004). Image Registration Using Hierarchical B-Splines. *IEEE Transactions on Visualization and Computer Graphics,* Vol.10, No.1, 2004, 85-94, ISSN:1077-2626
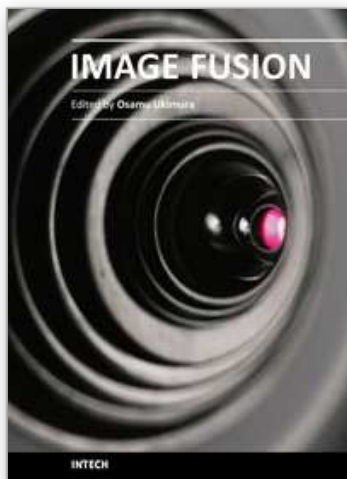
Image Fusion

Edited by Osamu Ukimura

ISBN 978-953-307-679-9

Hard cover, 428 pages

Publisher InTech

Published online 12, January, 2011

Published in print edition January, 2011

Image fusion technology has successfully contributed to various fields such as medical diagnosis and navigation, surveillance systems, remote sensing, digital cameras, military applications, computer vision, etc. Image fusion aims to generate a fused single image which contains more precise reliable visualization of the objects than any source image of them. This book presents various recent advances in research and development in the field of image fusion. It has been created through the diligence and creativity of some of the most accomplished experts in various fields.

How to reference

In order to correctly reference this scholarly work, feel free to copy and paste the following:

Bin Li (2011). Multimodal Medical Image Registration and Fusion in 3D Conformal Radiotherapy Treatment Planning, Image Fusion, Osamu Ukimura (Ed.), ISBN: 978-953-307-679-9, InTech, Available from: http://www.intechopen.com/books/image-fusion/multimodal-medical-image-registration-and-fusion-in-3d-conformal-radiotherapy-treatment-planning

INTECH

open science | open minds